

# Comparative Study of Dye-Sensitized Solar Cell Utilizing Seaweed and Rose Bengal Sensitizer: Influence of Dye Concentration

M.J. Jimmy<sup>1</sup>, A.M. Harun<sup>1,\*</sup>, M.Y.A. Rahman<sup>2,\*</sup>, N.A. Ludin<sup>3</sup>

<sup>1</sup> Faculty of Engineering, Universiti Malaysia Sabah, Jalan UMS, 88400, Kota Kinabalu, Sabah

<sup>2</sup> Institute of Microengineering and Nanoelectronics (IMEN), Universiti Kebangsaan Malaysia, 43600, Bangi, Selangor, Malaysia

<sup>3</sup> Solar Energy Research Institute (SERI), Universiti Kebangsaan Malaysia, 43600, Bangi, Selangor, Malaysia

\*E-mail: [mukifza@ums.edu.my](mailto:mukifza@ums.edu.my) (A.M. Harun); [mohd.yusri@ukm.edu.my](mailto:mohd.yusri@ukm.edu.my) (M.Y.A. Rahman)

Received: 6 December 2019 / Accepted: 20 January 2020 / Published: 10 March 2020

---

This work is concerned with the performance comparison study of dye-sensitized solar cell utilizing seaweed and rose bengal as dye-sensitizer. The influence of concentration of each dye on the optical absorption, photovoltaic performance and electrochemical impedance spectroscopy (EIS) data has been investigated. The 0.3 mM seaweed dye possesses the highest optical absorption. While, the 0.5 mM rose bengal dye exhibits the highest absorption in visible region. The DSSC utilizing the 0.3 mg/l seaweed dye produces the highest  $J_{sc}$  of 0.0183 mA cm<sup>-2</sup> due to the highest absorption in visible region and the lowest charge transfer resistance at the interface of Pt/electrolyte ( $R_{ct}$ ). The device using 0.5 mM rose bengal dye demonstrates the highest  $J_{sc}$  that is 0.1436 mA cm<sup>-2</sup> due to the highest absorption in visible region and the lowest charge transfer resistance at the interface of Pt/electrolyte. In conclusions, the performance of the device with rose bengal dye is higher than that of the device using seaweed dye. This is because the charge carrier lifetime of the device with rose bengal dye is longer than that of the device with seaweed dye. The power conversion efficiency of the device using both dyes is low.

---

**Keywords:** dye, dye-sensitized solar cell, rose bengal, seaweed, titanium dioxide

## 1. INTRODUCTION

Dye-sensitized solar cell (DSSC) is a third generation of solar cell that possesses advantage over first and second generation of solar cell. It has much lower fabrication cost than that of conventional silicon solar cell and thin film solar cell as first and second generation of solar cell, respectively. Nevertheless, the power conversion efficiency of the DSSC is lower than that of this first and second

generation of solar cell due to its optical absorption in visible region is lower than that of silicon solar cell and thin film solar cell. DSSC has three important components, namely, photoanode, electrolyte and cathode. The photoanode contains glass layer, conductive oxide layer, metal oxide film and dye as photosensitizer. Photoanode should possess high optical property to absorb much light in order to generate more electrons from highest molecular orbitals (HOMO) to lowest unoccupied molecular orbitals (LUMO) of dye molecules.

The most common dyes used in DSSC are organic and natural dyes. Synthetic dyes possess higher optical absorption than natural dye in visible region. Thus, the photovoltaic performance of the DSSC utilizing synthetic dyes is relatively higher than that of the device using natural dye. In [1], the DSSC utilizing naphthylphenylamine dye demonstrated the  $\eta$  of 7.08%. The DSSC employing carbazole-based dye performed the  $\eta$  as high as 9.37% compared to 8.17% that owned by the device using N719 dye [2]. In [3], it was reported that TiO<sub>2</sub> coated C218 sensitizer was used as a photoanode of DSSC that utilized cobalt sulphide counter electrode and cobalt-based redox electrolytes. This DSSC yielded the  $J_{sc}$  and  $\eta$  of 12.84 mA cm<sup>-2</sup> and 6.72%, respectively. Organic dye based on thioindigo was utilized as sensitizer of DSSC to produce the power conversion efficiency of 6.45% [4].

In [5], the DSSC using *Ixora* sp. (Rubiaceae) and *Canarium odontophyllum* as the natural dyes demonstrated the  $\eta$  of 0.96 and 0.59%, respectively. The corresponding  $J_{sc}$  were 6.26 and 2.45 mA cm<sup>-2</sup>, respectively. The DSSCs fabricated by using various natural dyes extracted from plant sources of *reseda luteola*, *berberis integerrima*, *panica granatum* pleniflora, *consolida orientalis*, *reseda gredensis*, *clematis orientalis*, *adonis flammea*, *salvia sclarea*, and *consolida ajacis* produced the  $J_{sc}$  in the range 0.04-0.68 mA cm<sup>-2</sup> [6]. The  $\eta$  obtained from these devices were low. The device utilizing natural dye extracted from *Azadirachta indica* performed quite high  $\eta$  that was 2.815 [7]. The DSSC based on papaya-leaf dye displayed the  $\eta$  0.28% [8].

This work is concerned with the comparative study of the performance of DSSC utilizing seaweed and rose bengal dye. The influence of each dye concentration on the performance of the device employing P25 TiO<sub>2</sub> as photoanode has been studied. The photovoltaic parameters are then correlated with the supporting data such as optical absorption, bulk resistance, charge transfer resistance and charge carrier lifetime of the device utilizing both dyes.

## 2. EXPERIMENTAL DETAILS

For preparation of P25 paste, 1 ml of ethanol, 2 ml of triton-x and 0.2 ml of poly(ethylene glycol) were poured in a bottle that contains 1 g of titanium (IV) oxide. The solution was put on a hot plate and stirred using magnetic stirrer for 1 hour at room temperature at 1200 rpm. For preparation of TiO<sub>2</sub> films, ITO substrates were firstly cleaned using acetone and ethanol in the right sequence in an ultrasonic bath. The TiO<sub>2</sub> layer was deposited on ITO substrates using a doctor blade technique. P25 paste was equally spread on the surface of conductive side ITO. A petri dish containing the paste coated on ITOs was then put on the hot plate for pre-heating process for 15 minutes at 100 °C. Next, it underwent annealing process at 400 °C for 1 hour in order to make sure the paste is strongly attached to ITO substrates. Finally, the TiO<sub>2</sub> films were formed.

The films were immersed in 0.1 mM seaweed dye solution for 24 hours at room temperature to ensure sufficient amount of dye molecules were adsorbed on the surface of the samples. The molecular formula of seaweed dye is  $C_{24}H_{18}O_4N_2$ . The IUPAC name of seaweed dye is -N-[4-[[4-(demethylamino)-phenyl] phenylmethylene] 2,5-cyclohexadienylidene] N-Methyl-methanaminium chloride. The prepared samples were employed as the photoanode for DSSC. This procedure was then repeated for preparing 0.2, 0.3, 0.4, 0.5 and 0.6 mM seaweed dye solution. On the other hand,  $TiO_2$  films were immersed in 0.1 mM rose bengal dye solution. This procedure was then repeated for preparing 0.2, 0.3, 0.4, 0.5 and 0.6 mM rose bengal dye solution. The molar mass of rose bengal dye is 973.67 g/mol and its molecular formula is  $C_{20}H_4Cl_4I_4O_5$ . Its IUPAC name is 4,5,6,7-tetrachloro-3',6'-dihydroxy-2',4',5',7'-tetraiodo-3*H*-Spiro [isobenzofuran-1,9'-xanthen]-3-one]. Both dyes were obtained from Universiti Teknologi Mara (UiTM). Both types of  $TiO_2$  coated dye samples underwent optical absorption characterization by UV-Vis spectrometer.

The counter electrode of the device was platinum film grown on ITO substrates via sputtering technique. Redox electrolyte containing iodide/triiodide was injected into the space between  $TiO_2$  coated N719 and platinum counter electrode. The devices with an illuminated area of  $0.23\text{ cm}^2$  were tested in dark and under illumination of  $100\text{ mW cm}^{-2}$  light. The light source used was tungsten halogen lamp. The electrochemical impedance spectroscopy (EIS) under illumination of  $100\text{ mW cm}^{-2}$  light was performed on the devices to determine the bulk resistance, charge transfer resistance and carrier transport time.

### 3. RESULTS AND DISCUSSION

Fig. 1 shows the UV-Vis spectra of  $TiO_2$  coated with seaweed dye with various dye concentrations. It is noticed that the optical absorption of the sample is significantly influenced by the concentration of seaweed dye. According to the figure, the 0.3 mg/l sample possesses higher optical absorption in UV region (300-400 nm) than in visible region (400-600 nm). For other samples, the absorption are about the same in the whole light spectrum. Also, according to the spectra, the 0.3 mg/l sample possess the highest absorption in the visible region, followed by 0.4, 0.5 and 0.2 mg/l samples in the descending order. The 0.1 and 0.6 mg/l share the lowest absorption.

Fig. 2 shows the UV-Vis spectra of  $TiO_2$  samples coated with rose bengal dye with various dye concentrations. According to the figure, the optical absorption of the sample is greatly influenced by the concentration of rose bengal dye. The 0.5 mM sample has the highest absorption followed by 0.6, 0.4, 0.3, 0.2 and 0.1 mM samples in the descending order. For 0.5 mM sample, its absorption in visible region is higher than that in UV region reflected by a wavelength peak at 560 nm. This sample also shows an absorption peak at 310 nm. The absorption in 600-700 nm region is smaller than that in UV and other visible region. For 0.6 M sample, it possesses higher absorption in UV region than visible region. For other samples, the absorption is almost similar in the whole spectrum.

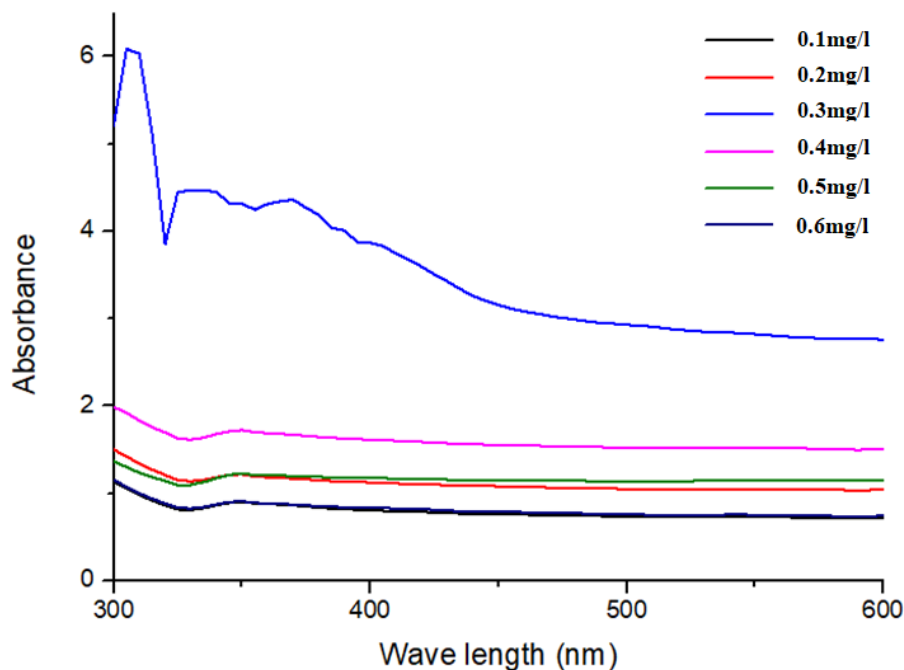


Figure 1. UV-Vis absorption for seaweed dye with various concentrations

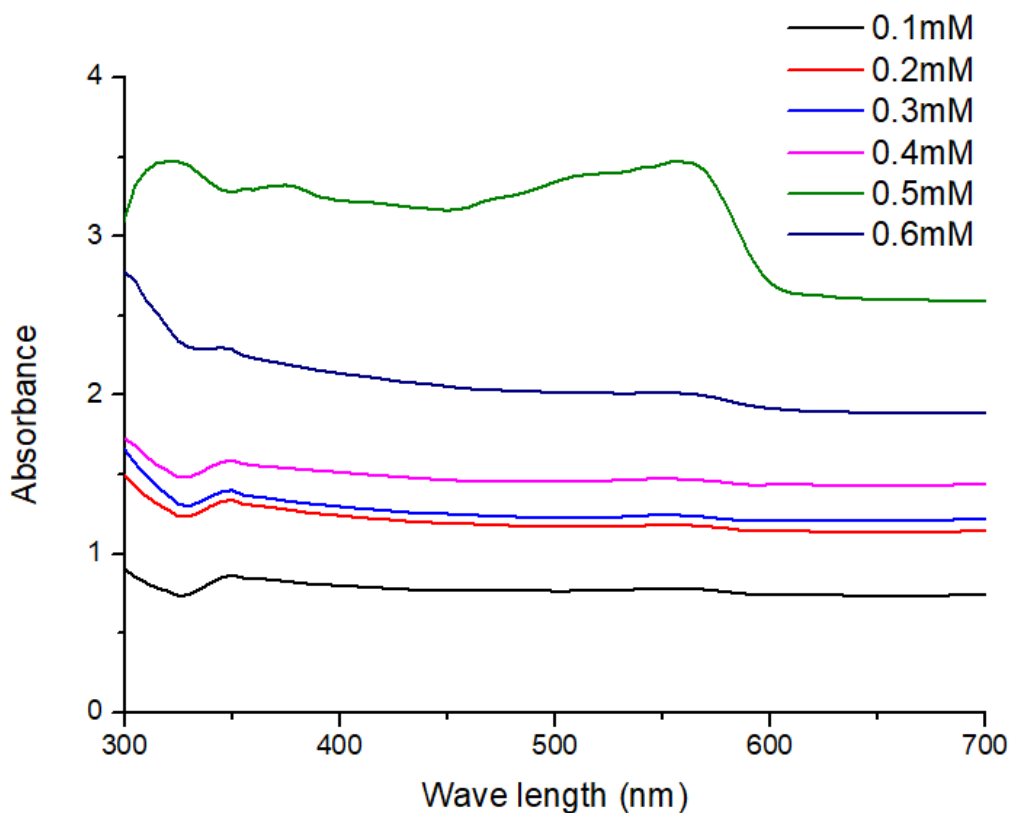
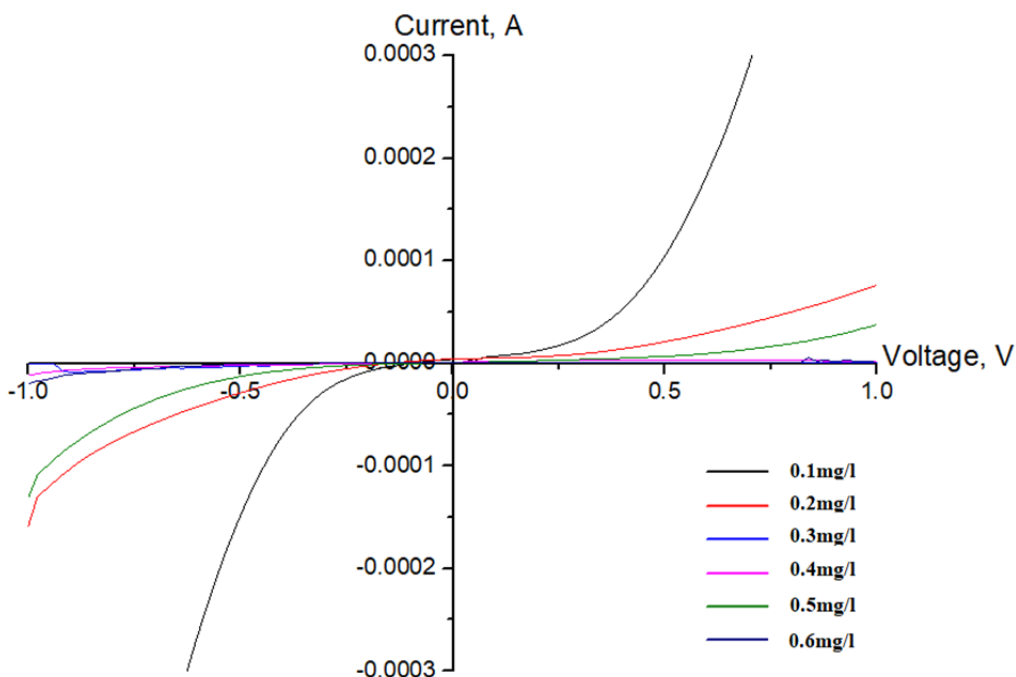


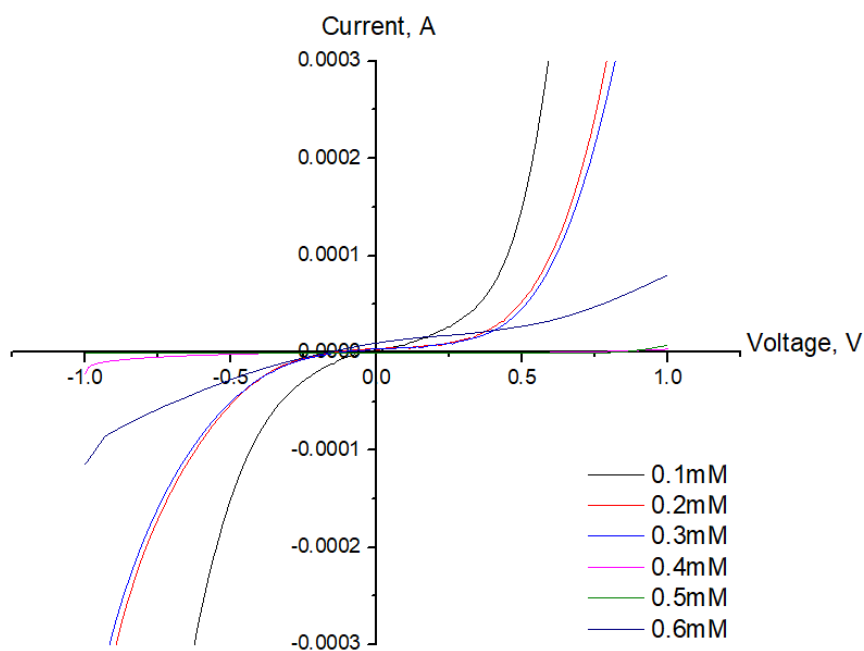
Figure 2. UV-Vis absorption for rose bengal dye with various concentrations

Fig. 3 shows the *I-V* curves in dark of the DSSC utilizing TiO<sub>2</sub> coated with seaweed dye with various concentrations. According to the figure, the leak current which is also the current in reverse bias is quite similar to the forward current for all devices. It is because the reverse current curves are symmetry with the forward current curves. The device utilizing the 0.1 mg/l sample has the highest

forward current, followed by 0.2, 0.5 and other samples. The forward current in the device using the other samples, namely, 0.3, 0.4 and 0.6 mg/l samples is small and can be observed from the figure. It is concluded that the forward current decreases with the concentration of seaweed dye. While, the device utilizing the 0.4 mg/l sample possesses the lowest leak current, followed by 0.3, 0.5, 0.2 and 0.1 mg/l samples. It is observed that there is no increasing nor decreasing trend of the leak current with the concentration of seaweed dye.



**Figure 3.** *I-V* in dark for the devices with various concentrations of seaweed dye



**Figure 4.** *I-V* curves in dark for the devices using rose bengal dye with various concentrations

Fig. 4 shows the *I-V* curves in dark of the DSSC utilizing TiO<sub>2</sub> coated with rose bengal dye with various dye concentrations. The reverse current is almost similar to the forward current for all devices since the reverse current curves are symmetry with the forward current curves. In other words, the devices do not show rectification property, signifying that the current is not dominant in one direction [9]. According to Fig. 4, the device with 0.1 mM sample owns the highest forward current at the lowest voltage, followed by the device with 0.2 and 0.3 mM sample. This phenomena is not seen for the other devices. It is expected that the devices will exhibit low photocurrent if they do not show rectification property.

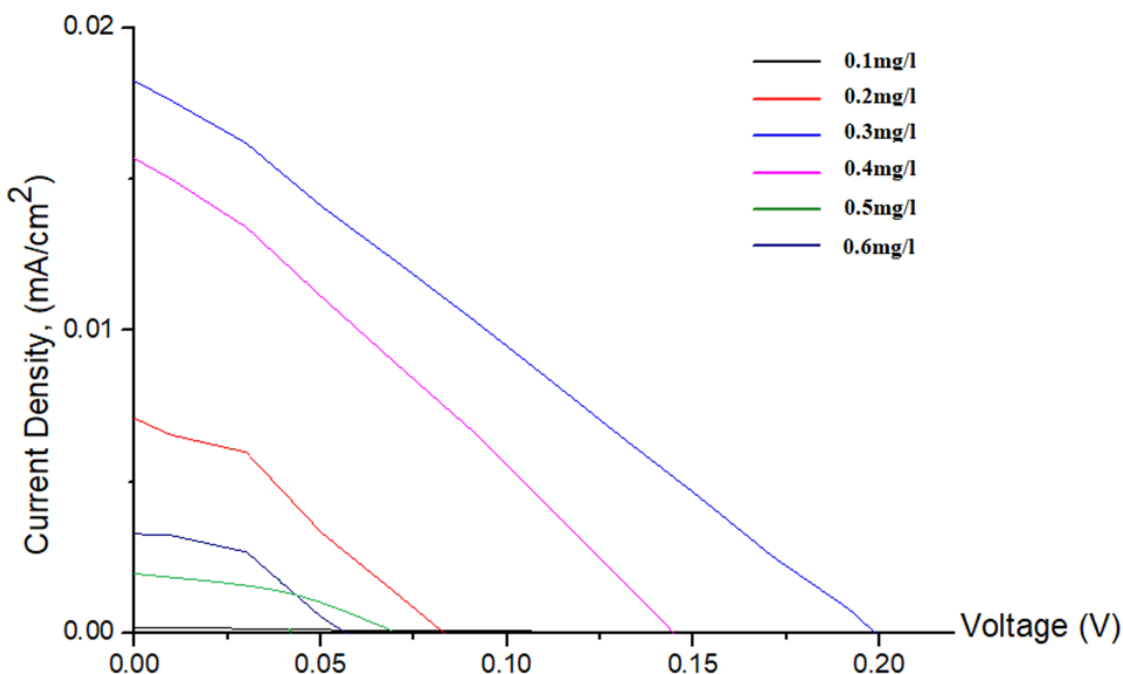


Figure 5. *J-V* curves under illumination with various concentrations of seaweed dye

Table 1. Photovoltaic parameters of DSSC with various concentrations of seaweed dye

| Concentration (mg/l) | V <sub>oc</sub> (V) | J <sub>sc</sub> (mA/cm <sup>2</sup> ) | FF    |
|----------------------|---------------------|---------------------------------------|-------|
| 0.1                  | 0.141               | 0.0002                                | 0.294 |
| 0.2                  | 0.081               | 0.0071                                | 0.313 |
| 0.3                  | 0.202               | 0.0183                                | 0.256 |
| 0.4                  | 0.141               | 0.0157                                | 0.282 |
| 0.5                  | 0.070               | 0.0056                                | 0.548 |
| 0.6                  | 0.060               | 0.0033                                | 0.407 |

Fig. 5 shows the *J-V* curves under illumination of the DSSC utilizing TiO<sub>2</sub> coated seaweed dye with various concentrations. From the figure, the shape of the curve for the device utilizing the 0.3 and 0.4 mg/l samples are almost straight line. This indicates that the internal resistance in the devices is very high, lowering the photocurrent in the devices. The straight line curve has been reported in the solar cell

with the structure ITO/TiO<sub>2</sub>/PVC-LiClO<sub>4</sub>/graphite [10,11]. However, the shape of the curve for the device employing the 0.2 and 0.6 mg/l sample is not straight line. Interestingly, the shape of the curve of the device with 0.5 mM follows the ideal shape of *J-V* curve of solar cell [12, 13]. The photovoltaics parameters are analyzed from Fig. 5 and illustrated in Table 1.

Fig. 6 depicts the *J-V* curves under illumination of the devices employing TiO<sub>2</sub> coated rose bengal with various concentrations. It is clearly seen that the shape of the curve for all devices are straight line [14]. This tells us that the current decreases fastly with the voltage as shown in Fig. 6. The internal resistance in these devices is very high, reducing the current in the devices upon light illumination. It is observed that the device with the 0.3 mM sample produces the highest output power, followed by the devices with the 0.4, 0.2, 0.6, 0.5 and 0.1 mM samples in descending order. The photovoltaics parameters are extracted from Fig. 6 and listed in Table 2.

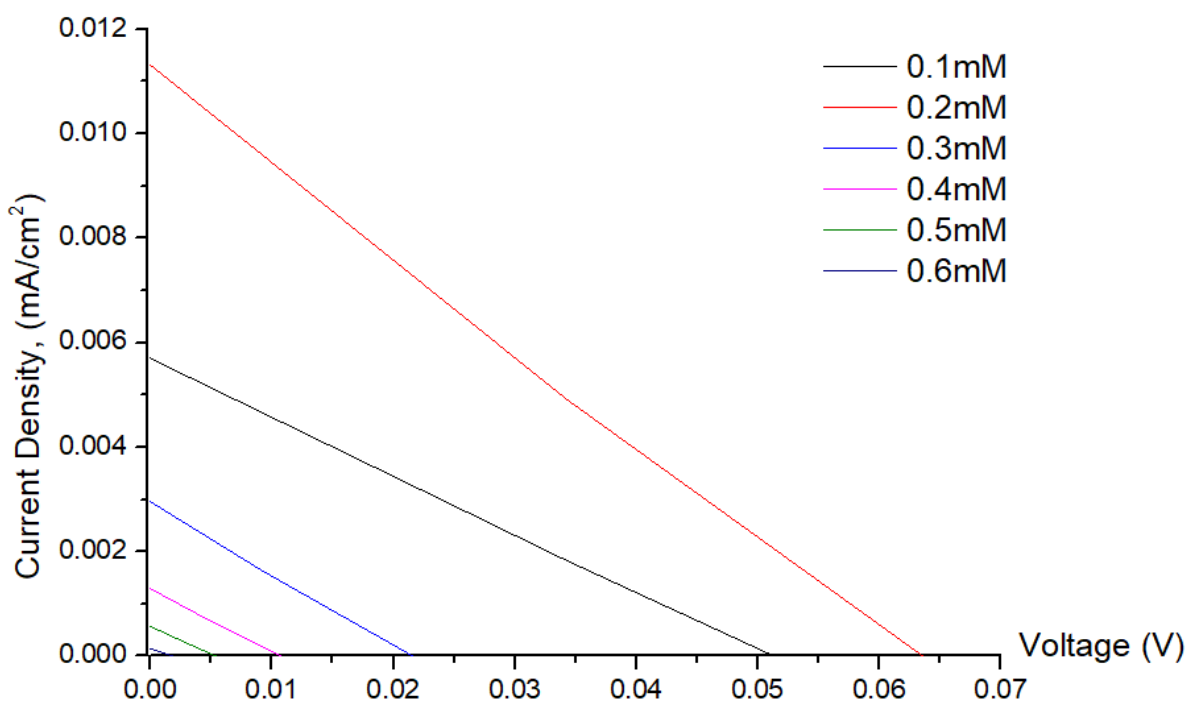


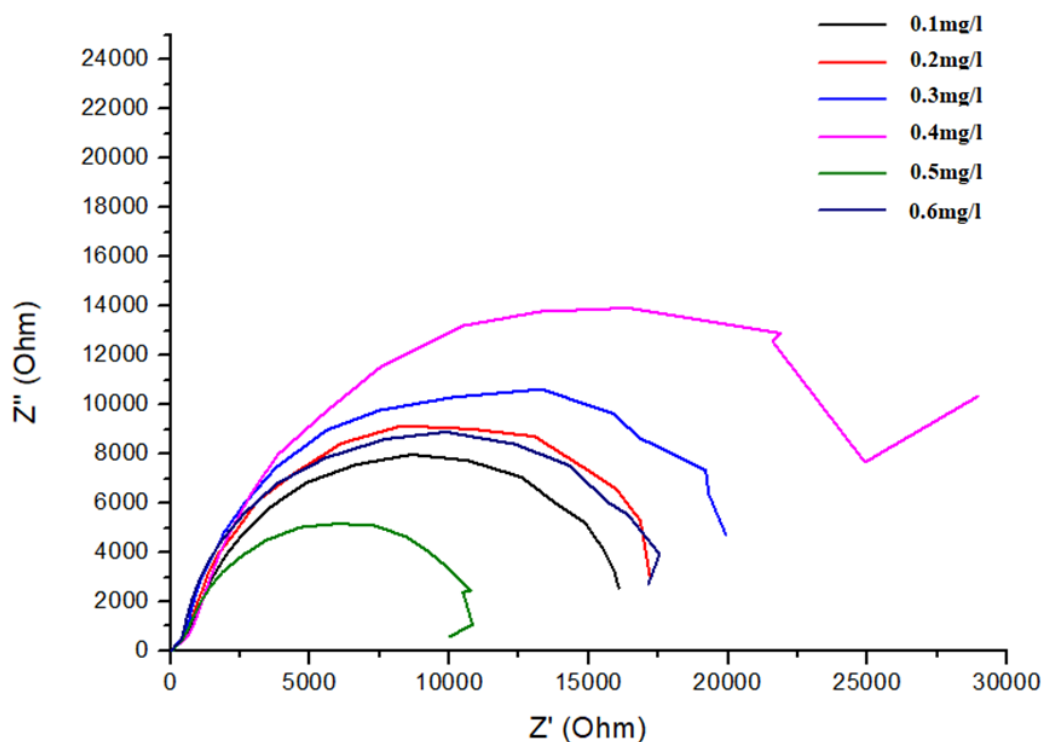
**Figure 6.** *J-V* curves under illumination with various concentrations of rose bengal dye

**Table 2.** Photovoltaic parameters of DSSC utilizing rose bengal dye with various concentrations

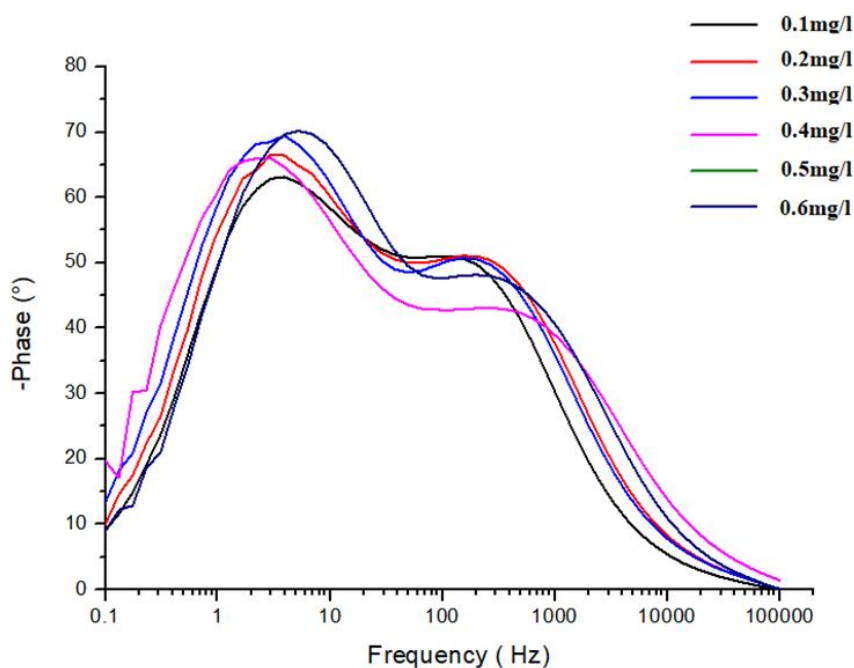
| Concentration (mM) | <i>V</i> <sub>oc</sub> (V) | <i>J</i> <sub>sc</sub> (mA/cm <sup>2</sup> ) | <i>FF</i> |
|--------------------|----------------------------|--|-----------|
| 0.1                | 0.0688                     | 0.0057                                       | 0.160     |
| 0.2                | 0.1378                     | 0.0113                                       | 0.108     |
| 0.3                | 0.1378                     | 0.0108                                       | 0.151     |
| 0.4                | 0.1377                     | 0.0251                                       | 0.236     |
| 0.5                | 0.2756                     | 0.1436                                       | 0.216     |
| 0.6                | 0.1378                     | 0.0236                                       | 0.228     |

Fig. 7 depicts the Nyquist plots under illumination of the DSSC using TiO<sub>2</sub> coated seaweed dye with various dye concentrations. According to the plots, there is only semicircle representing the charge transfer resistance at the interface of Pt/electrolyte ( $R_{ct}$ ). A straight line which is not observed from Fig. 7 originating from origin to starting point of the semicircle represents the bulk resistance of the device ( $R_b$ ). The frequency corresponding with the straight line region is higher than that of semicircle region. These two resistances are listed in Table 3. According to the table, it is noticeable that the  $R_{ct}$  is much higher than  $R_b$ , telling that the charge carriers moves much slower at the interface of Pt/electrolyte than within the device. It is found that the  $R_{ct}$  for all devices are high, which lowers down the  $J_{sc}$  significantly as listed in Table 1. The device employing the 0.3 mg/l dye owns the lowest  $R_{ct}$ , followed by the device using 0.2, 0.4, 0.5, 0.1 and 0.6 mg/l seaweed dye. While, the device with 0.1 mg/l seaweed dye has the lowest  $R_b$ , followed by the device with 0.5, 0.4, 0.3, 0.2 and 0.6 mg/l samples.

Fig. 8 displays the Bode plots under illumination of the devices using seaweed dye with various concentrations. The plots show two peaks, however, the maximum frequency denoted by the highest peak is only used to compute the carrier lifetime ( $\tau$ ) and also presented in Table 3. In [15], it was reported that the bode plot of the DSSC utilizing Ag doped rGO displays two peaks. The device with 0.6 mg/l sample owns the longest  $\tau$  followed by the device with 0.5, 0.1, 0.4, 0.2 and 0.3 mg/l seaweed dye in the descending order. However, the device with 0.5 and 0.1 mg/l dyes share the same  $\tau$ . According to Table 1, the device employing the 0.3 mg/l sample demonstrates the highest  $J_{sc}$ . However, this device does not own the smallest  $R_b$  and the longest  $\tau$ .



**Figure 7.** Nyquist plots for the devices with various concentrations of seaweed dye



**Figure 8.** Bode plots for the devices with various concentrations of seaweed dye

The device with the smallest  $R_b$  and the longest  $\tau$  should perform the highest  $J_{sc}$ . However, this device has the smallest  $R_{ct}$ . This means that this device allows the charge carrier to travel the fastest at the interface of Pt/electrolyte. The fastest triiodide is reduced to iodide. The highest  $J_{sc}$  owned by the device with the 0.3 mg/l sample can be caused by another factor such as by the highest optical absorption in the visible region as shown in Fig. 1. The  $TiO_2$  coated seaweed dye samples with the highest light absorption in the visible region generate the largest number of electrons from the highest occupied molecular orbitals (HOMO) level to the lowest unoccupied molecular orbitals (LUMO) level. Thus, the highest number of electrons are then donated to the conduction band of  $TiO_2$  which serves as an electron acceptor. On the other hand, the device with 0.1 mg/l sample demonstrates the lowest  $J_{sc}$  due to the lowest absorption in the visible region.

**Table 3.** EIS Parameters of DSSC using seaweed dye with various concentrations

| Concentration (mg/l) | $R_b(\Omega)$ | $R_{ct}(\Omega)$ | $\tau$ (s) |
|----------------------|---------------|------------------|------------|
| 0.1                  | 59            | 17444            | 0.193      |
| 0.2                  | 89            | 9924             | 0.146      |
| 0.3                  | 86            | 7503             | 0.110      |
| 0.4                  | 83            | 10504            | 0.192      |
| 0.5                  | 74            | 11729            | 0.193      |
| 0.6                  | 137           | 17561            | 0.256      |

Fig. 9 depicts the Nyquist plots under illumination of the devices utilizing  $TiO_2$  coated rose bengal dye with various concentrations. According to the plots, there is only a semicircle representing the charge transfer resistance at the interface of Pt/electrolyte ( $R_{ct}$ ), similar to that of the devices with seaweed dye. A straight line representing bulk resistance ( $R_b$ ) is not observed from Fig. 9. These two

resistances are presented in Table 4. It is found that the  $R_{ct}$  for all devices are high, similar to the case of the devices with seaweed dye which decreases the  $J_{sc}$  significantly as illustrated in Table 2. According to Table 4, the device with 0.6 mM sample owns the lowest  $R_b$ , followed by the device with 0.3, 0.2, 0.4, 0.5 and 0.1 mM sample in the ascending order. For  $R_{ct}$ , the device with 0.5 mM sample possesses the lowest value, followed by 0.1, 0.2, 0.3, 0.6 and 0.4 mM sample in the ascending order.

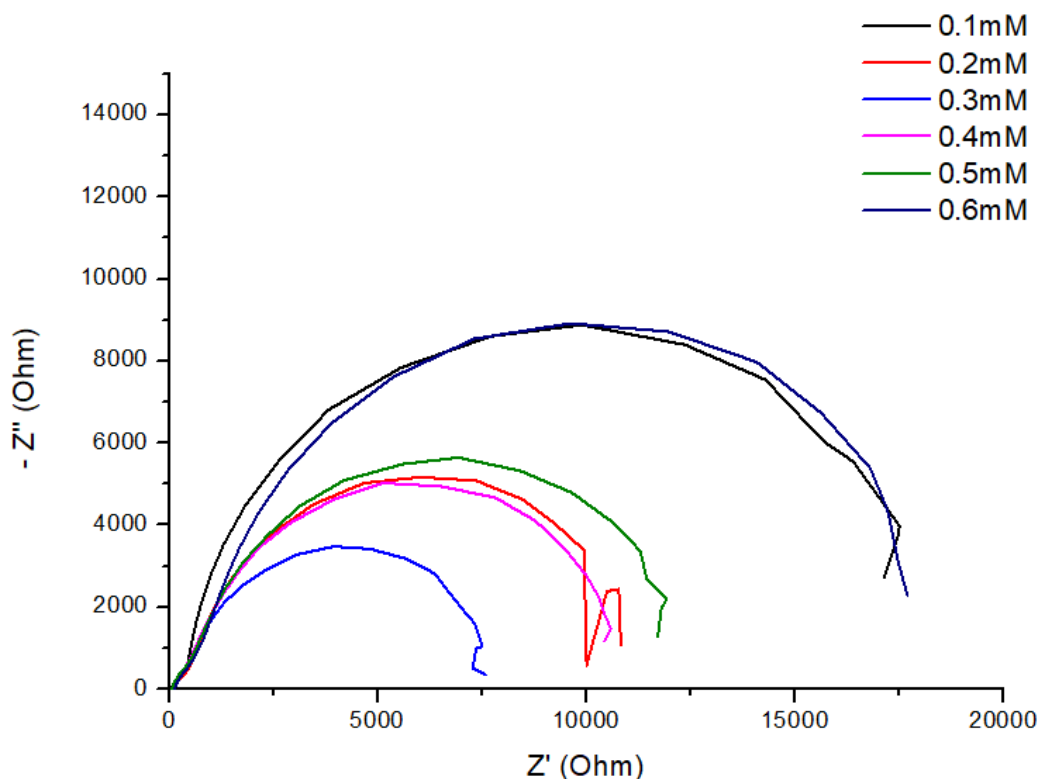


**Figure 9.** Nyquist plots for the devices using various rose bengal dye with various concentrations

Fig. 10 displays the Bode plots under illumination of the devices with various concentrations of rose bengal. The plots show two peaks, however, the maximum frequency denoted by the highest peak is only used to compute the carrier lifetime ( $\tau$ ) and also presented in Table 4. The device with 0.4 mM sample owns the longest  $\tau$  followed by the device with 0.2, 0.3, 0.1, 0.6 and 0.5 mM dye in the descending order. However, the device with 0.2 and 0.3 mM dyes share the same  $\tau$ . According to Table 2, the device employing the 0.5 mM sample demonstrates the highest  $J_{sc}$  of  $0.1436 \text{ mA cm}^{-2}$ . This  $J_{sc}$  value is comparable with that reported in [6]. However, this device does not own the smallest  $R_b$  and the longest  $\tau$  as illustrated in Table 4. However, this device has the smallest  $R_{ct}$ . The highest  $J_{sc}$  owned by the device with the 0.5 mM sample can be caused by another factor such as by the highest optical absorption in the visible region as shown in Fig. 2.

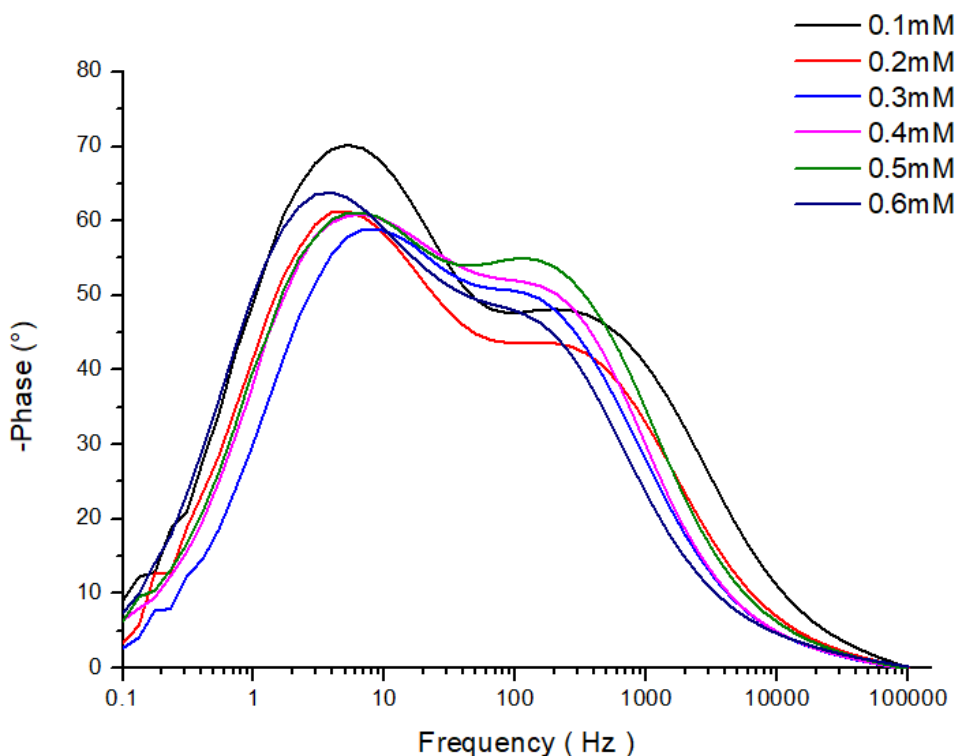


Figure 10. Bode plots for the devices with various concentrations of rose bengal

Table 4. EIS Parameters of DSSC utilizing rose bengal dye with various concentrations

| Concentration (mM) | $R_b$ ( $\Omega$ ) | $R_{ct}$ ( $\Omega$ ) | $\tau$ (s) |
|--------------------|--------------------|-----------------------|------------|
| 0.1                | 96                 | 15981                 | 0.256      |
| 0.2                | 71                 | 17119                 | 0.339      |
| 0.3                | 69                 | 19856                 | 0.339      |
| 0.4                | 82                 | 28859                 | 0.450      |
| 0.5                | 89                 | 9924                  | 0.189      |
| 0.6                | 59                 | 17444                 | 0.254      |

Table 5 illustrates the performance of the DSSC utilizing various natural dyes in term of short-circuit current density ( $J_{sc}$ ). It is noticed that the device with neem dye performed the highest  $J_{sc}$  while that using seaweed dye produced the lowest  $J_{sc}$ . This might be due to neem and seaweed dye possessed the highest and lowest optical absorption in the visible region, respectively.

Table 5. Performance of DSSC utilizing various natural dyes

| Dye                           | $J_{sc}$ (mA/cm <sup>2</sup> ) | Reference |
|-------------------------------|--------------------------------|-----------|
| Seaweed                       | 0.02                           | This work |
| Rose bengal                   | 0.14                           | This work |
| <i>Ixora</i> sp. (Rubiaceae)  | 6.26                           | [5]       |
| <i>Canarium odontophyllum</i> | 2.45                           | [5]       |
| <i>Reseda luteola</i>         | 0.04                           | [6]       |
| <i>Consolida ajacis</i>       | 0.68                           | [6]       |

|                     |       |      |
|---------------------|-------|------|
| Neem                | 15.10 | [7]  |
| Bixin               | 1.10  | [16] |
| Annato              | 0.53  | [16] |
| Norbixin            | 0.38  | [16] |
| Mangosteen pericarp | 2.54  | [17] |
| Rhododendron        | 1.52  | [17] |
| Black rice          | 1.14  | [18] |
| Spinach             | 0.46  | [19] |
| Ipomoea             | 0.91  | [19] |
| Rossela             | 1.63  | [20] |
| Blue pea            | 0.37  | [20] |

#### 4. CONCLUSIONS

The influence of seaweed dye and rose bengal concentration on the DSSC performance has been compared. It is found that the DSSC utilizing rose bengal dye performed higher photocurrent than that of the device with seaweed dye. The device utilizing 0.3 mg/l seaweed dye performed the highest  $J_{sc}$  of 0.0183 mA cm<sup>-2</sup> due to the highest absorption in the visible region and lowest charge transfer resistance at the interface of Pt/electrolyte. The device using 0.5 mM rosebengal dye produced the highest  $J_{sc}$  of 0.1436 mA cm<sup>-2</sup> due to the same reasons of the device with seaweed dye.

#### ACKNOWLEDGEMENTS

The authors would like to thank UKM for providing financial assistance under a research grant FRGS/1/2019/STG02/UKM/02/1 and GUP-2018-081 for carrying out this work.

#### References

1. Y.J. Chang and T.J. Chow, *Tetrahedron*, 65 (2009) 4726.
2. A. El-Shafei, M. Hussain, A. Atiq, A. Islam and L. Han, *J. Mater. Chem.*, 22 (2012) 24048.
3. S.K. Swami, N. Chaturvedi, A. Kumar, R. Kapoor, V. Dutta, J. Frey, T. Moehl, M. Grätzel, S. Mathew, M.K. Nazeeruddin, *J. Power Sources*, 275 (2015) 80.
4. M. Hossiennezad, S. Moradian and K. Gharanjig, *Dyes and Pigments*, 123 (2015) 147.
5. N.T.R.N. Kumara, P. Ekanayake, A. Lim, L.Y.C. Liew, M. Iskandar, L.C Ming, G.K.R. Senadeera, *J. Alloys Comp.*, 581 (2013) 186.
6. M. Hamadaniyan, S. Ghomi, M. Hosseinpour, R. Masoomi and V. Jabbari, *Mater. Sci. Sem. Process.*, 27 (2014) 733.
7. S. Sahare, N. Veldurthi, R. Singh, A.K. Swarnkar, M. Salunkhe and T. Bhave, *Mat. Res. Exp.*, 2 (2015) 10.
8. S. Suyitno, T.S. Saputra, A. Supriyanto and Z. Arifin, *Spectrochim. Acta Part A*, 148 (2015) 99.
9. M.Y.A Rahman, M.M Salleh, I.A. Talib and M. Yahaya, *Curr. Appl. Phys.*, 5 (2005) 599.
10. M.Y.A Rahman, M.M. Salleh, I.A. Talib and A. Ahmad, *Curr. Appl. Phys.*, 7 (2007) 446.
11. M.Y.A Rahman, M.M. Salleh and I.A. Talib, *Ionics*, 13 (2007) 241.
12. M.Y.A. Rahman, S.A.M. Samsuri and A.A. Umar, *Appl. Phys. A*, 125 (2019) 59.
13. S.N. Sadikin, M.Y.A. Rahman and A.A. Umar, *Superlatt. Microstruct.*, 130 (2019) 153.
14. M.Y.A. Rahman, M.M. Salleh, I.A. Talib and M. Yahaya, *J. Power Sources*, 133 (2004) 293.
15. N. Mustaffa, M.Y.A. Rahman and A.A. Umar, *Ionics*, 24 (2018) 3665.
16. N.M. Gomez-Ortiz, I.A. Vazquez-Maldonado, A.R. Perez-Espadas, G.J. Mena-Rejon, J.A. Azamar-Barrios and G. Oskam, *Sol. Energy Mater. Sol. Cells*, 94 (2010) 40.

17. H. Zhou, L. Wu, Y. Gao and T. Ma, *J. Photochem. Photobiol A*, 219 (2011) 188.
18. S. Hao, J. Wu, Y. Huang and J. Lin, *Sol. Energy*, 80 (2006) 209.
19. H. Chang, H.M. Wu, T.L. Chen, K.D. Huang, C.S. Jwo and Y.J. Lo, *J. Alloys. Compd.*, 495 (2010) 606.
20. K. Wongcharee, V. Meeyoo and S. Chavadej, *Sol. Energy Mater. Sol. Cells*, 91 (2007) 566.

© 2020 The Authors. Published by ESG ([www.electrochemsci.org](http://www.electrochemsci.org)). This article is an open access article distributed under the terms and conditions of the Creative Commons Attribution license (<http://creativecommons.org/licenses/by/4.0/>).